



## Hierarchical patterns with sub-20 nm pattern fidelity via block copolymer self-assembly and soft nanotransfer printing

Journal:	<i>Polymer Chemistry</i>
Manuscript ID	PY-ART-03-2019-000335.R1
Article Type:	Paper
Date Submitted by the Author:	04-May-2019
Complete List of Authors:	Tran, Helen; Stanford University, Chemical Engineering Bergman, Harrison; Columbia University, Chemistry Parenti, Kaia; Columbia University, Chemistry van der Zande, Arend; University of Illinois at Urbana-Champaign, Mechanical Science and Engineering Dean, Cory; Columbia University, Physics Campos, Luis; Columbia University, Chemistry



## Hierarchical patterns with sub-20 nm pattern fidelity via block copolymer self-assembly and soft nanotransfer printing

Helen Tran<sup>a,†</sup>, Harrison M. Bergman<sup>a,§</sup>, Kaia Parenti<sup>a</sup>, Arend M. van der Zande<sup>b,||</sup>, Cory R. Dean<sup>c</sup>, and Luis M. Campos<sup>a,\*</sup>

Received 00th January 20xx,  
Accepted 00th January 20xx

DOI: 10.1039/x0xx00000x

www.rsc.org/

We describe the development of a technique to transfer micrometer patterns of organic thin films with sub-50 nm edge resolution and sub-20 nm pattern fidelity. Large-area transfer of homopolymers, diblock copolymers, and small molecules films is demonstrated, and extended to multitudes of different shapes. Moreover, this technique is amenable to sequential printing (i.e. multilayer stacking) and can be integrated with 2D atomic crystals. This high-fidelity pattern transfer work has broad scope for its potential uses from the construction of Van der Waals heterostructures interfaced with self-assembled block copolymer thin films to the development of platforms to investigate the influence of hierarchical patterning on cell differentiation.

### Introduction

Constructing complex patterns is broadly pertinent for fabricating electronic devices, modeling biological systems, and developing materials possessing emergent properties beyond their constituent components.<sup>1–10</sup> Critical challenges include the realization of order across both the micrometer and nanometer regimes and interfacing with organic materials both as a building element and heterogeneous substrate. For instance, in the field of tissue engineering, mimicking the complex biological architecture pervasive in natural systems requires the patterning of proteins at multiple length scales. In developing methods to fabricate hierarchically ordered patterns, simplicity and reliability enable the technique to be easily adopted by researchers across diverse disciplines.

Block copolymer self-assembly induced by solvent annealing is a powerful and versatile technique to impart microphase segregation, leading to nanoscale feature sizes across an entire thin film. Key parameters to tune long range order and domain orientation include solvent selection, time, vapor pressure, quenching environments, and temperature.<sup>11</sup> Notably, solvent annealing may mitigate preferential substrate interactions and allows the decoupling between the substrate and resulting self-assembly to some degree. This decoupling may be tempered by

macroscopic topographical heterogeneities. While deliberate templating may be leveraged to generate long-range ordering,<sup>1,12</sup> surface defects may adversely damage the thin film integrity and yield dewetted samples. This is particularly relevant for adopting solvent-vapor-induced block copolymer self-assembly on undefined and rough samples, such as exfoliated 2D materials. A key challenge is the decoupling the solvent-vapor-induced block copolymer self-assembly from the target application. Moreover, in order to generate hierarchical patterns, the thin films must be lithographically processed (which may not be compatible with upstream processes) or a specialized block copolymer must be synthesized. For example, in order to achieve hierarchical patterns with block copolymers, we reported the introduction of a photo-crosslinkable brominated styrene handle.<sup>13</sup> A more versatile method applicable to a wide range of block copolymers without the need for synthesis is desirable. Thus, techniques based on thin film transferring have gained attention.

Nanotransfer printing, which often employs elastomeric stamps and relies on surface chemistries (i.e. adhesion), has enabled the assembly of complex constructs and the effective integration of heterogeneous materials.<sup>14–19</sup> Such techniques allow the high-fidelity printing of a broad class of inks (e.g. inorganic nanostructures, 2D materials, biopolymers, etc.) for applications in flexible electronics, biosensors, optoelectronics, and other devices.<sup>20–27</sup> Inks are transferred from the donor substrate and printed to the final substrate by carefully engineering the competing van der Waals forces between the stamp and substrate,<sup>18,28</sup> relative strength of the adhesive,<sup>29,30</sup> or kinetics of the peeling.<sup>31,32</sup> Unusual 3D architectures, large-scale arrays,<sup>33</sup> and stacks of cross-solubility layers<sup>34</sup> have been straightforwardly generated via nanotransfer printing.

Several versions of nanotransfer printing have been reported, each with modifications to target a limitation in substrate compatibility or processability. Seminal work by Loo

<sup>a</sup> Department of Chemistry, Columbia University, New York, NY, 10027.

<sup>b</sup> Department of Mechanical Engineering, Columbia University, New York, NY, 10027.

<sup>c</sup> Department of Physics, Columbia University, New York, NY, 10027.

<sup>†</sup> Currently at Chemical Engineering, Stanford University.

<sup>§</sup> Currently at Chemistry, University of California—Berkeley

<sup>||</sup> Currently at Mechanical Engineering, University of Illinois, Urbana-Champaign.

Electronic Supplementary Information (ESI) available: Additional AFM and optical images and photographs of transfer process. See DOI: 10.1039/x0xx00000x

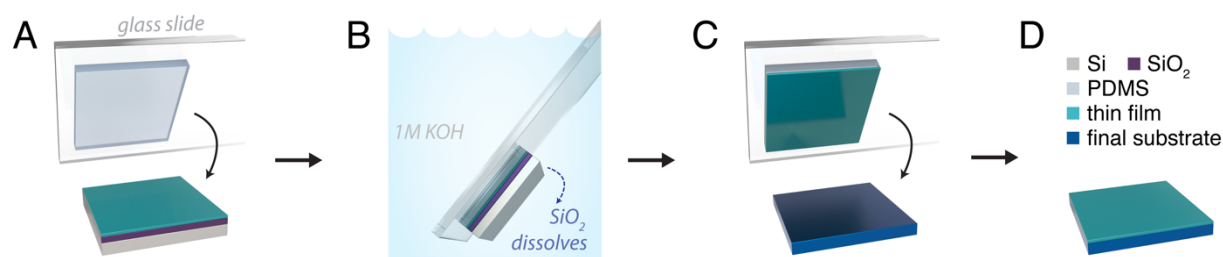


Figure 1. Overall schematic for soft pattern-transfer printing. (A) A PDMS stamp attached to a glass slide is placed in direct contact with the thin film on interest, which was prepared on SiO<sub>2</sub>/silicon, and (B) soaked in 1M KOH until the SiO<sub>2</sub> dissolves. (C) After the silicon substrate detaches upon SiO<sub>2</sub> etching, the thin film is transferred to the PDMS and (D) placed in direct contact with the final substrate.

and Rogers and colleagues described the use of thiol-terminated self-assembled monolayers (SAMs) to covalently transfer gold patterns from the relief structures of micropatterned polydimethylsiloxane (PDMS) stamps.<sup>18,26,35</sup> Many iterations have focused on replacing SAMs with an interfacial layer that serves as a gentle release mechanism to widen the types of materials that may be transferred.<sup>29,36–39</sup> Alternatively, exploiting kinetically controlled adhesion eliminates the need for SAMs and adhesive layers altogether.<sup>32</sup> Though so-called universal methods have been reported, each transfer technique possesses merits and drawbacks in terms of relative transfer rate, resolution, processing ease, and scope of materials accessible.<sup>38</sup> For instance, Park and colleagues report a patterned taping approach that is stimuli-free (*i.e.* no heat or pressure), cost-efficient, and time efficient; however it suffers from poor resolution compared to previous literature with edge resolution on the order of micrometers as opposed to nanometers. For specifically exploiting the nanoscale features obtained through block copolymer self-assembly, Nealey and coworkers developed molecular transfer printing.<sup>40,41</sup> Thin films of ternary blends of a block copolymers and two reactive end-functionalized homopolymers self-assemble on a master substrate, typically with chemical or physical cues for long-range ordering. A final substrate (*i.e.* where the pattern is desired) is placed in contact with the self-assembled ternary blend and the homopolymer inks are transferred via absorption, chemical reaction or some other attractive interaction. In this approach, careful attention is placed on ensuring the self-assembly of the ternary blends yields the appropriate morphology where each homopolymer ink must concentrate in its respective block copolymer domains. The degree of importance for each parameter determines which method is best suited for a particular application.

Inspired by the collective advances in nanotransfer printing, we aimed to develop a simple, yet effective method tailored for transferring thin films of organic materials, principally self-assembled block copolymers, with high resolution, which enables patterning at multiple length scales simultaneously, termed soft pattern-transfer printing (Fig. 1). In particular, soft pattern-transfer printing is useful for the transfer of thin films that undergo substrate dependent processing. For example, the adoption of SAM-based transfer methods requires that the films are prepared on hydrophobic surfaces, such as a monolayer of octyltrimethyl silane, in order for the for Van der Waals

interactions to be appropriately engineered for transfer. However, solvent annealing of block copolymer thin films on hydrophobic surfaces often leads to dewetting of the thin film with solvent swelling. In contrast to molecular transfer printing, we aimed to develop a method where established self-assembled block copolymer systems can be directly used without the need of optimizing a new ternary system. The method begins with a film on silicon dioxide, a standard substrate used for thin film preparation, particularly for block copolymers, minimizing the need to optimize self-assembly processing. We exploit the fact that silicon dioxide is slowly etched by base to universally transfer films from the substrate to PDMS, obviating the need to consider the relative Van der Waals interactions between the parent and second substrate. This technique is commonly used in other laboratory procedures, such as the preparation of thin films for Transmission Electron Microscopy (TEM), and we expect its adoption would be easily executed by a wide range of researchers. Notably, the thin film must be stable in water and base, excluding the applicability of this method for systems such as water-soluble polyelectrolytes. Moreover, we aimed for the use of basic tools, minimal expertise, and no thermal evaporators, thereby contributing to its accessibility to researchers outside the field of block copolymer self-assembly and use in high-throughput applications. Analogous to other transfer printing methods, thin films function as the “ink” and thus do not suffer from surface diffusion or edge disorder. We demonstrate the successful large-area transfer of small molecules, homopolymers, and diblock copolymers. The need for nanotransfer printing is illustrated by transferring self-assembled diblock copolymer films on top of 2D atomic crystals, which are challenging substrates for solvent vapor assisted annealing due to the presence of crystal edges and residue. Interfacing self-assembled block copolymers and 2D materials may lead to emergent properties, such as improved catalytic behavior in the hydrogen evolution reaction or capability to extend the refractive index of transparent materials.<sup>42–44</sup> However, the interface of block copolymers and 2D atomic crystals is limited to small grain sizes or more complicated processing.<sup>44–47</sup> Moreover, we demonstrate hierarchical structures through nanoscale patterning with the self-assembled diblock copolymers and a micropatterns with a micropatterned PDMS stamp. Sub-50 nm edge resolution and sub-20 nm pattern fidelity is achieved. Finally, we show the

technique can also be used iteratively, with sequential printing leading to the construction of complex patterns or layered systems.

## Results and discussion

The overall schematic for soft pattern-transfer printing is illustrated in Fig. 1, with accompanying optical images of the process in Fig. S1. Thin films are prepared on silicon with silicon dioxide ( $\text{SiO}_2$ ) as the sacrificial layer. In the optical images, a thin film of regioregular poly(3-hexylthiophene-2,5-diyl) (P3HT) was prepared on 280 nm  $\text{SiO}_2$  for visualization purposes (Fig. S1A). In the case of self-assembled block copolymers, processing such as thermal or solvent annealing is completed at this stage. A glass slide is cleaned in oxygen plasma for two minutes before the PDMS stamp is placed to increase adhesion and avoid detachment during the following steps. The rigid glass slide provides structural stability for manipulation of the sample without distorting the PDMS stamp, which in turn would deform the transferred thin film. The PDMS and thin film are gently placed in direct contact, uniformly without the presence of air bubbles (Fig. 1a, S1a-b). The complex is submerged in 1M potassium hydroxide (KOH), which etches the sacrificial  $\text{SiO}_2$  layer between the thin film and silicon substrate, until the underlying substrate detaches (Fig. 1b, S1c). As a result, the thin film remains in direct contact with the PDMS (Fig. S1d). Then, the newly-attached thin film on PDMS is placed in direct contact with the final substrate and may be lightly heated (70°C, 10 seconds) to ensure conformal printing (Fig. 1c-d, S1e-f). Conformal printing is confirmed by imaging with atomic force microscopy (AFM), where sub-nanometer height differences are observed over a 10 micrometer region of poly(methyl methacrylate) (PMMA) thin film that was printed with soft pattern-transfer printing (Fig. S2).

We select polystyrene-*ortho*-nitrobenzyl-polyethylene oxide (PS-*hv*-PEO) for an initial study because it contains a useful photocleavable linker that allows PEO to be selectively removed to yield a nanoporous thin film.<sup>48,49</sup> Upon solvent annealing on silicon dioxide on silicon substrates, thin films of PS-*hv*-PEO phase segregate into perpendicular 15 nm PEO cylinders in a matrix of PS and exhibit micron-scale long-range ordering. Thin films are subjected to UV irradiation to cleave the *o*-nitrobenzyl unit and rinsed with methanol/water to remove the PEO phase, resulting in a nanoporous PS thin film, as observed with AFM (Fig. 2a, S3a). After undergoing soft pattern-transfer printing, the fidelity of the nanopatterns is retained, as observed by AFM (Fig. 2b, S3b). Note, minimal pressure is applied during contact to avoid distortion of the PDMS stamp. Too much pressure applied damages the thin film, with cracks appearing when imaged with AFM, despite macroscopically appearing as a uniform thin film (Fig. S4a-b). Similar nanopattern fidelity and pressure sensitivity results were observed with PS-*b*-PEO and PS-*b*-PEO-biotin.

As previously alluded to, soft pattern-transfer printing is well suited for instances where thin film processing is incompatible with the final substrate, such as diblock copolymer self-assembly on 2D atomic crystals. For instance, molybdenum

disulfide samples ( $\text{MoS}_2$ , Figure 2C) prepared by chemical vapor deposition (CVD) showed thin film dewetting upon solvent vapor annealing (Figure 2D). During solvent vapor annealing, the block copolymer thin film detaches and surface tension of the swelled film delaminates the  $\text{MoS}_2$  crystals, revealing the underlying purple silicon dioxide (Figure 2D). This problem is exacerbated with exfoliated samples, which are often preferred over CVD-grown samples due to ease of preparation and high quality of mono and few-layer flakes. The presence of tape residue and thick flakes presents a challenge to achieve uniform spin-coated films and long-range ordering.

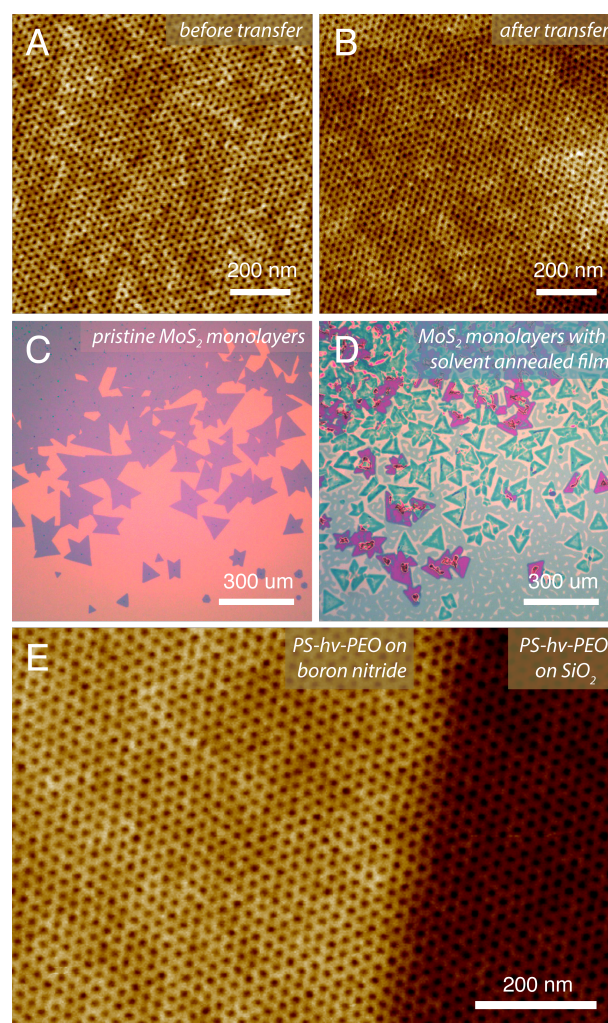


Figure 2. AFM images of thin films of PS-*hv*-PEO show that the nanopatterns imaged (A) before transfer are retained (B) after soft pattern-transfer printing. Optical images show (C) pristine monolayer  $\text{MoS}_2$  prepared by CVD, and (D) the sample after spin-coating a film of PS-*hv*-PEO and solvent annealing. Delamination, as seen as the purple triangles and clumped regions, occurs. (E) AFM image of a BN flake edge with a thin film of PS-*hv*-PEO transferred on top. The left, higher region is the BN flake and the right, lower region is  $\text{SiO}_2$ .

Self-assembly via solvent annealing on 2D materials is possible but is unreliable and limited to smaller sub-micron grain boundaries and a higher density of defects (Fig. S5a-c). To realize larger grain size, the solvent annealing time is typically increased, but this also results in increased dewetting (Fig. S6).

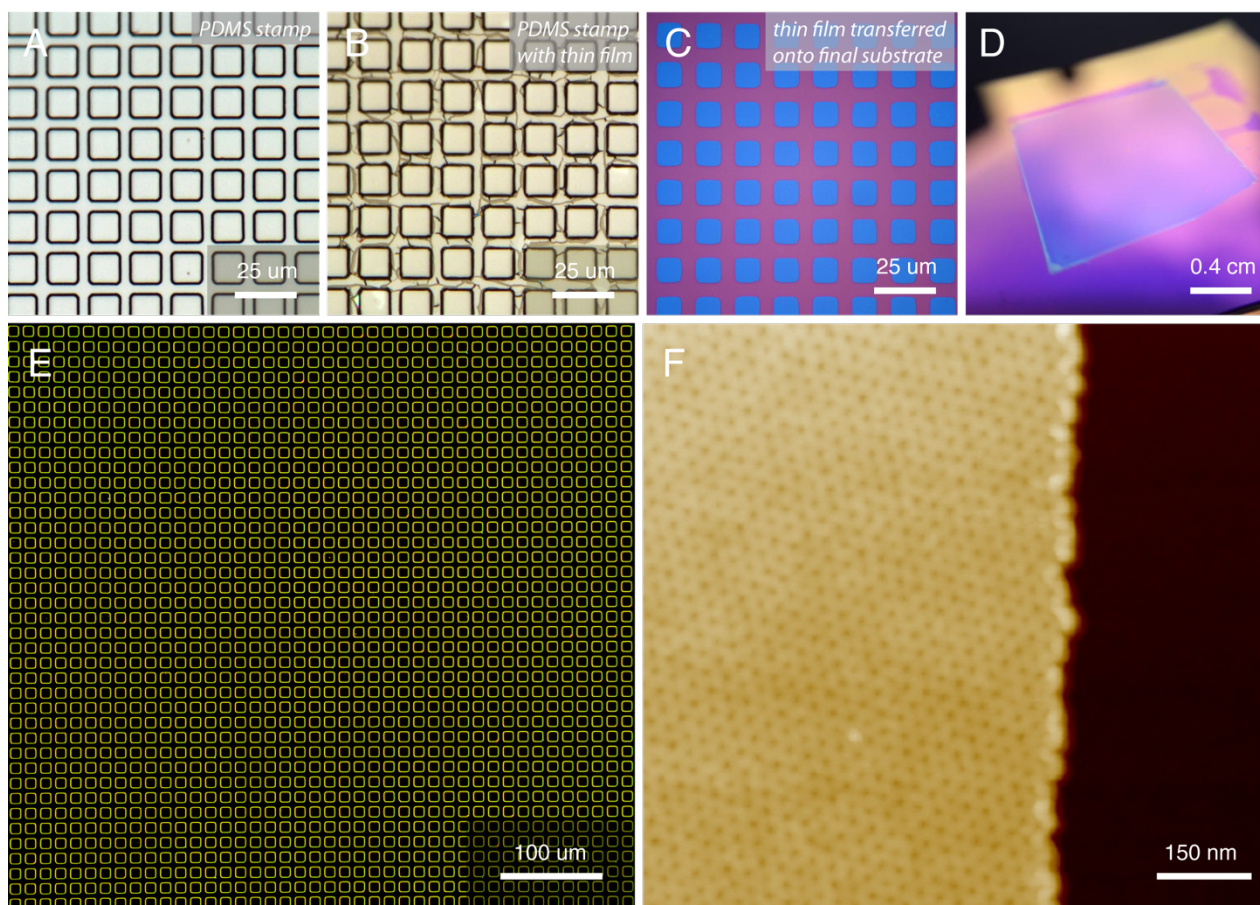


Figure 3. Soft pattern-transfer printing with a micropatterned PDMS stamp. (A) A PDMS stamp is prepared with raised  $10\ \mu\text{m}$  squares spaced  $5\ \mu\text{m}$  apart. (B) A thin film of PS-*h*v-PEO is transferred on top of the PDMS stamp, and the deformed film can be seen in the regions between the squares. (C) A bright-field optical image of the printed PS-*h*v-PEO square arrays (D) over a one-centimeter chip is shown. (E) Dark field imaging and (F) AFM reveals well-defined edges with high fidelity of pattern transfer.

An optical image shows a uniform diblock copolymer film spin-coated on a boron nitride flake on  $\text{SiO}_2$  (Fig. S6a), which separates at the boron nitride flake edge and gathers in the center after solvent annealing (Fig. S6b). Phase segregation is observed on the  $\text{SiO}_2$  substrate, but not on the boron nitride flake (Fig. S6c). Hence, the transfer of well-ordered self-assembled thin films of diblock copolymers onto 2D atomic crystals is an attractive application for soft-pattern transfer printing. Accordingly, we transferred well-ordered thin films of PS-*h*v-PEO, which were self-assembled on blank  $\text{SiO}_2$ , on top of boron nitride flakes (Fig. 2e). The left, higher region of the AFM image is a thin film of PS-*h*v-PEO on top of a  $15\ \text{nm}$  flake of BN and the right, lower region of the AFM image is a thin film of PS-*h*v-PEO on  $\text{SiO}_2$ . Although the edge of an exfoliated flake is not commonly used for device fabrication, we noticed that the edge of the BN flake is slightly less resolved compared to before the transfer, exhibiting  $\sim 50\ \text{nm}$  edge resolution. This alludes to the limit of conformal contact between the atomic crystal and block copolymer thin film. The minor curvature of the thin film lead to a slight increase in edge resolution, as expected. Similar to previous transfers onto a bare  $\text{SiO}_2$  substrate, well-defined nanopatterns on the BN flake is observed.

The use of a micropatterned PDMS stamp, rather than a flat uniform stamp, extends the utility of soft pattern-transfer

printing (Figure 3). A PDMS stamp with an array of  $10\ \mu\text{m}$  squares and  $5\ \mu\text{m}$  pitch was prepared from a silicon master (Fig. 3a). Examination of the PDMS stamp after the transfer of thin films (see step in Fig. 1c, S1, S1d) shows no optically visible features on the relief square regions where the film is in contact conformably, and film deformation and cracks in the depressed regions in between the squares (Fig. 3b). We demonstrate soft pattern-transfer printing with thin films of small molecules (a perylene diimide derivative, Fig. S8), homopolymers (P3HT, Fig. S9), and block copolymers (PS-*h*v-PEO, Fig. 3c). Well-defined square arrays on millimeter length scales are observed by bright field microscopy (Fig. 3d, S7, S8c, S9c) and dark field microscopy (Fig. 3e). Analogous to previously published techniques, micropatterns of organic thin films were printed in a straightforward and high-throughput manner, with resolution comparable to the best techniques to date and feature sizes down to  $10\ \mu\text{m}$ .

Notably, soft pattern-transfer printing of self-assembled nanostructured diblock copolymer films with a micropatterned PDMS leads to hierarchical patterning, where micropatterns derive from the PDMS shapes and nanopatterns from the diblock copolymer self-assembly. An AFM image of the edge of a transferred square of PS-*h*v-PEO shows the micrometer-sized film with nanometer-sized features, with approximately  $20\ \text{nm}$

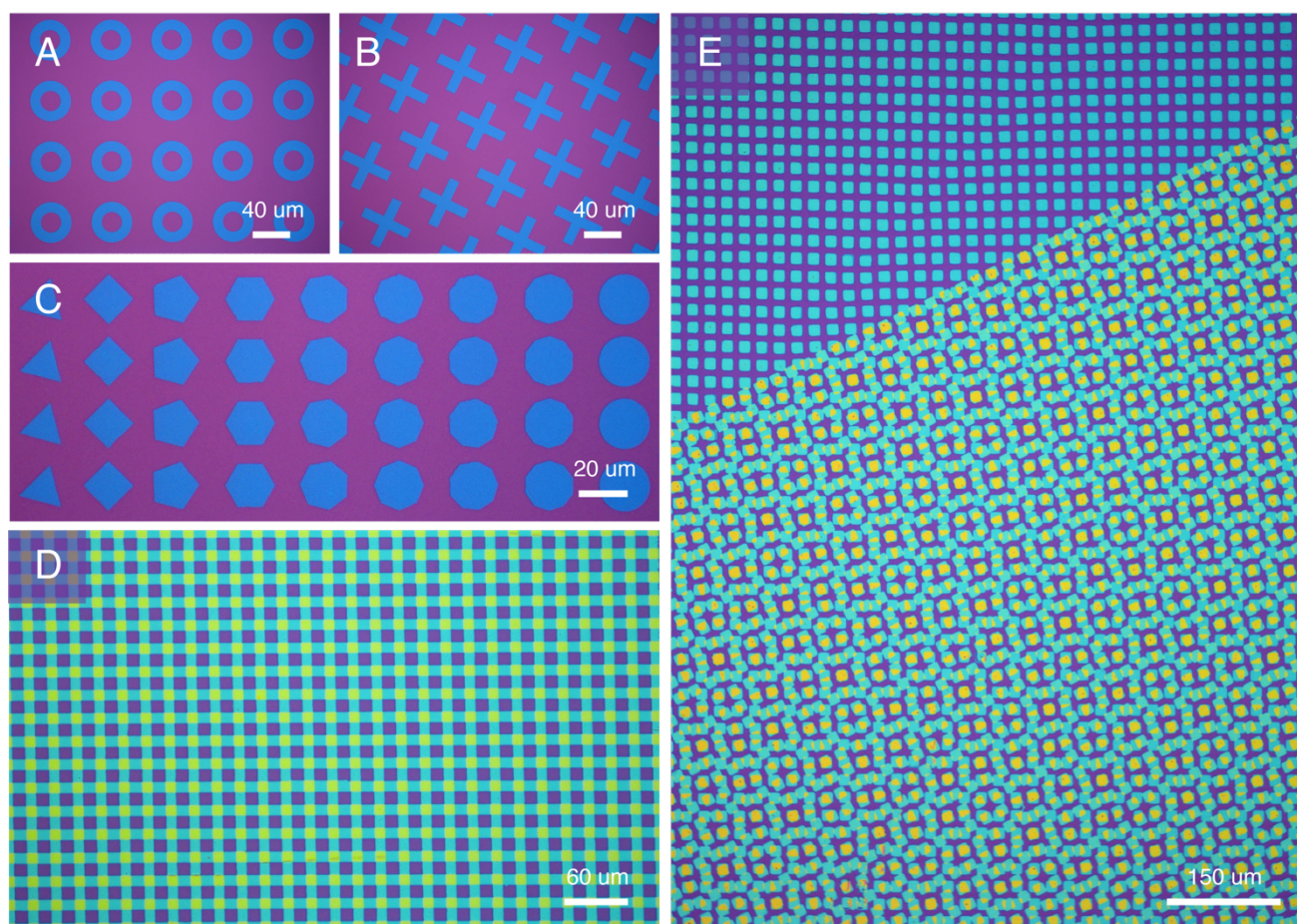


Figure 4. Shape and sequential printing study. Thin films of PS-hv-PEO is printed with (A) ring and (B) cross array stamps. (C) A polygon study shows an array of triangles to decagons and a circle printed, with corner definition reduced after an octagon for 20  $\mu\text{m}$  shapes. (D) Sequential printing is demonstrated by first printing an array of lines, then printing a second array of lines  $90^\circ$  relative to the first set. (E) Sequential printing is demonstrated by first printing an array of squares, then printing a second array of lines approximately  $4^\circ$  relative to the first set. The purple regions are  $\text{SiO}_2$ , the green regions are single layer of P3HT, and the yellow regions are double layer of P3HT.

edge resolution (Figure 3f). Soft pattern-transfer printing of nanostructured diblock copolymer films with a micropatterned PDMS is a viable strategy for hierarchical patterning, particularly for biomolecules with sub-50 nm features where limited high-throughput strategies are currently available. For instance, we previously published the synthesis of poly(styrene-*co*-bromostyrene)-block-poly(ethylene oxide)-biotin [P(S-*co*-BrS)-*b*-PEO-biotin], where bromostyrene functions as the UV-active unit allowing selective crosslinking of thin films to fabricate micropatterns.<sup>13</sup> With our soft pattern-transfer printing method, we can directly transfer PS-*b*-PEO-biotin, the non-crosslinkable control version without bromostyrene, to obtain substrates for hierarchical biomolecule patterning and conveniently avoid the need to synthesize an entirely new polymeric system (Fig. S10). This serves as a potential strategy to hierarchically pattern biomolecules with sub-50 nm resolution by effectively extending the utility of biologically relevant diblock copolymers.<sup>50,51</sup>

The examples presented so far feature an array of squares with rounded corners for soft-pattern transfer printing; however, this technique is not limited to squares, and more complex shapes may be transferred with similarly high fidelity. By designing a different master for the PDMS molds, shapes

such as lines (Fig S11), rings (Fig. 4a), crosses (Fig. 4b, S12a), and circles (Fig. S12b), can be transferred in a similar fashion. The rings demonstrate that non-filled shapes can be transferred, while sharp  $90^\circ$  edges are observed in the crosses (Fig. 4b). Moreover, a study on the number of sides in a polygon was conducted (Fig. 4c), where the number of sides increased from 3 to 10 and a circle. We observe that the polygon shapes are clearly defined up to an octagon for 20  $\mu\text{m}$  dimensions and begins to lose its corner definition for the nonagons and decagons. We anticipate that the nonagon and decagon may be resolved with larger shape sizes.

Similar to other printing techniques,<sup>15</sup> sequential printing is also demonstrated, where a thin film is printed on top of an existing printed pattern. These multilayered structures may lead to emergent physical properties and the progress of 3D integrated organic circuits.<sup>52–54</sup> Here, we show sequential printing with an array of lines (Fig. 4d) and squares (Fig. 4e). First, an array of squares or lines is printed, then a second printing at a different angle results in a complex pattern (Fig. S13). For the line patterns, we printed the second layer at  $90^\circ$  relative to the first layer of lines to yield a mesh of single layers of P3HT (Fig. 4d, blue regions) but double layers where the lines intersect (Fig. 4d, yellow regions). For the square arrays, both

the single layer and double layer of printing may be simultaneously observed (Fig. 4e). Complex structures may be sequentially built up, and theoretically transferred again. In fact, such patterns resemble Moiré patterns, which are frequently observed in Nature and have gained interest in the research community, which may be utilized to create complex patterns of local physical and electronic perturbations.

## Conclusions

Driven by the need to transfer organic materials with high resolution and hierarchical control on non-homogenous substrates, we developed a nanotransfer technique termed soft pattern-transfer printing which does not rely on adhesive layers nor external stimuli, leading to a cost and time efficient high throughput processing scheme. Representative organic thin films of P3HT homopolymers, self-assembled diblock copolymers (e.g. PS-*h*v-PEO, PS-*b*-PEO-biotin), and functionalized perylene diimide small molecules were employed as inks for micron-sized arrays of patterns ranging from squares, lines, polygons, and rings. Notably, micron-sized arrays of self-assembled block copolymers yielded hierarchical patterns, where the nanoscale patterns derived from the block copolymers added a level of patterning. Moreover, to build layers of complex structures onto the same film, the technique can be repeated through sequential printing. This technique may have implications in the development of 2D bioactive platforms to study the effects of cellular differentiation on size and patterns and allows the interface of Van der Waals heterostructures with self-assembled thin films of block copolymers. In the future, we envision that soft pattern-transfer printing will allow more researches to achieve high throughput patterning of organic materials with high resolution while accessing complex hierarchical patterns onto hybrid materials with highly complex patterns and architectures.

## Conflicts of interest

There are no conflicts to declare.

## Acknowledgements

H.T. is currently supported by an appointment to the Intelligence Community Postdoctoral Research Fellowship Program at Stanford University, administered by Oak Ridge Institute for Science and Education through an interagency agreement between the U.S. Department of Energy and the Office of the Director of National Intelligence. K.P. thanks the Department of Defense (DoD) for a National Defense Science & Engineering Graduate (NDSEG) Fellowship. Superlattice patterning of transition metal dichalcogenides was partially supported by Office of Naval Research (ONR) Young Investors Program (no. N00014-17-1-2832)

## Notes and references

- 1 I. Bita, J. K. W. Yang, Y. S. Jung, C. A. Ross, E. L. Thomas and K. K. Berggren, *Science*, 2008, **321**, 939–943.
- 2 K. A. Kilian, B. Bugarija, B. T. Lahn and M. Mrksich, *PNAS*, 2010, **107**, 4872–4877.
- 3 R. Ruiz, H. Kang, F. A. Detcheverry, E. Dobisz, D. S. Kercher, T. R. Albrecht, J. J. de Pablo and P. F. Nealey, *Science*, 2008, **321**, 936–939.
- 4 D. E. Discher, D. J. Mooney and P. W. Zandstra, *Science*, 2009, **324**, 1673–1677.
- 5 M. J. Dalby, N. Gadegaard, R. Tare, A. Andar, M. O. Riehle, P. Herzyk, C. D. W. Wilkinson and R. O. C. Oreffo, *Nat Mater*, 2007, **6**, 997–1003.
- 6 T. Dvir, B. P. Timko, D. S. Kohane and R. Langer, *Nat Nano*, 2011, **6**, 13–22.
- 7 J. K. W. Yang, Y. S. Jung, J.-B. Chang, R. A. Mickiewicz, A. Alexander-Katz, C. A. Ross and K. K. Berggren, *Nat Nano*, 2010, **5**, 256–260.
- 8 S. Zhang, *Nat Biotech*, 2003, **21**, 1171–1178.
- 9 K. Na, C. Jo, J. Kim, K. Cho, J. Jung, Y. Seo, R. J. Messinger, B. F. Chmelka and R. Ryoo, *Science*, 2011, **333**, 328–332.
- 10 S. Yim, S. Jeon, J. M. Kim, K. M. Baek, G. H. Lee, H. Kim, J. Shin and Y. S. Jung, *ACS Appl. Mater. Interfaces*, 2018, **10**, 2216–2223.
- 11 B. C. Stahl, E. J. Kramer, C. J. Hawker and N. A. Lynd, *Journal of Polymer Science Part B: Polymer Physics*, 2017, **55**, 1125–1130.
- 12 H. M. Jin, D. Y. Park, S.-J. Jeong, G. Y. Lee, J. Y. Kim, J. H. Mun, S. K. Cha, J. Lim, J. S. Kim, K. H. Kim, K. J. Lee and S. O. Kim, *Advanced Materials*, 2017, **29**, 1700595.
- 13 H. Tran, K. Ronaldson, N. A. Bailey, N. A. Lynd, K. L. Killops, G. Vunjak-Novakovic and L. M. Campos, *ACS Nano*, 2014, **8**, 11846–11853.
- 14 M. Ikawa, T. Yamada, H. Matsui, H. Minemawari, J. Tsutsumi, Y. Horii, M. Chikamatsu, R. Azumi, R. Kumai and T. Hasegawa, *Nat Commun*, 2012, **3**, 1176.
- 15 J. W. Jeong, S. R. Yang, Y. H. Hur, S. W. Kim, K. M. Baek, S. Yim, H.-I. Jang, J. H. Park, S. Y. Lee, C.-O. Park and Y. S. Jung, *Nat Commun*, 2014, **5**, 5387.
- 16 E. Menard, L. Bilhaut, J. Zaumseil and J. A. Rogers, *Langmuir*, 2004, **20**, 6871–6878.
- 17 A. L. Briseno, M. Roberts, M.-M. Ling, H. Moon, E. J. Nemanick and Z. Bao, *J. Am. Chem. Soc.*, 2006, **128**, 3880–3881.
- 18 Y.-L. Loo, R. L. Willett, K. W. Baldwin and J. A. Rogers, *Applied Physics Letters*, 2002, **81**, 562–564.
- 19 J. Zaumseil, M. A. Meitl, J. W. P. Hsu, B. R. Acharya, K. W. Baldwin, Y.-L. Loo and J. A. Rogers, *Nano Lett.*, 2003, **3**, 1223–1227.
- 20 M. S. Onses, C. Song, L. Williamson, E. Sutanto, P. M. Ferreira, A. G. Alleyne, P. F. Nealey, H. Ahn and J. A. Rogers, *Nature Nanotechnology*, 2013, **8**, 667–675.
- 21 K.-B. Lee, S.-J. Park, C. A. Mirkin, J. C. Smith and M. Mrksich, *Science*, 2002, **295**, 1702–1705.
- 22 W.-S. Liao, S. Cheunkar, H. H. Cao, H. R. Bednar, P. S. Weiss and A. M. Andrews, *Science*, 2012, **337**, 1517–1521.
- 23 J. Song, F.-Y. Kam, R.-Q. Png, W.-L. Seah, J.-M. Zhuo, G.-K. Lim, P. K. H. Ho and L.-L. Chua, *Nat Nano*, 2013, **8**, 356–362.
- 24 M. J. Allen, V. C. Tung, L. Gomez, Z. Xu, L.-M. Chen, K. S. Nelson, C. Zhou, R. B. Kaner and Y. Yang, *Adv. Mater.*, 2009, **21**, 2098–2102.
- 25 C. H. Lee, D. R. Kim and X. Zheng, *PNAS*, 2010, **107**, 9950–9955.

- 26 Y.-L. Loo, T. Someya, K. W. Baldwin, Z. Bao, P. Ho, A. Dodabalapur, H. E. Katz and J. A. Rogers, *PNAS*, 2002, **99**, 10252–10256.
- 27 B. Hwang, S.-H. Shin, S.-H. Hwang, J.-Y. Jung, J.-H. Choi, B.-K. Ju and J.-H. Jeong, *ACS Appl. Mater. Interfaces*, 2017, **9**, 27351–27356.
- 28 J. B. Kim, S. Lee, M. F. Toney, Z. Chen, A. Facchetti, Y. S. Kim and Y.-L. Loo, *Chem. Mater.*, 2010, **22**, 4931–4938.
- 29 K. Sim, S. Chen, Y. Li, M. Kammoun, Y. Peng, M. Xu, Y. Gao, J. Song, Y. Zhang, H. Ardebili and C. Yu, *Scientific Reports*, 2015, **5**, 16133.
- 30 H. Yi, M. Seong, K. Sun, I. Hwang, K. Lee, C. Cha, T. Kim and H. E. Jeong, *Advanced Functional Materials*, 2018, **28**, 1706498.
- 31 X. Feng, M. A. Meitl, A. M. Bowen, Y. Huang, R. G. Nuzzo and J. A. Rogers, *Langmuir*, 2007, **23**, 12555–12560.
- 32 M. A. Meitl, Z.-T. Zhu, V. Kumar, K. J. Lee, X. Feng, Y. Y. Huang, I. Adesida, R. G. Nuzzo and J. A. Rogers, *Nat Mater*, 2006, **5**, 33–38.
- 33 R. F. Tiefenauer, K. Tybrandt, M. Aramesh and J. Vörös, *ACS Nano*, 2018, **12**, 2514–2520.
- 34 A. Abdellah, A. Falco, U. Schwarzenberger, G. Scarpa and P. Lugli, *ACS Appl. Mater. Interfaces*, 2016, **8**, 2644–2651.
- 35 Y.-L. Loo, R. L. Willett, K. W. Baldwin and J. A. Rogers, *J. Am. Chem. Soc.*, 2002, **124**, 7654–7655.
- 36 K.-H. Kim, K.-W. Bong and H. H. Lee, *Applied Physics Letters*, 2007, **90**, 093505.
- 37 S. Y. Park, T. Kwon and H. H. Lee, *Advanced Materials*, 2006, **18**, 1861–1864.
- 38 S. Oh, S. K. Park, J. H. Kim, I. Cho, H.-J. Kim and S. Y. Park, *ACS Nano*, 2016, **10**, 3478–3485.
- 39 J. W. Jeong, W. I. Park, L.-M. Do, J.-H. Park, T.-H. Kim, G. Chae and Y. S. Jung, *Adv. Mater.*, 2012, **24**, 3526–3531.
- 40 S. Ji, C.-C. Liu, G. Liu and P. F. Nealey, *ACS Nano*, 2010, **4**, 599–609.
- 41 T. Inoue, D. W. Janes, J. Ren, H. S. Suh, X. Chen, C. J. Ellison and P. F. Nealey, *Advanced Materials Interfaces*, 2015, **2**, 1500133.
- 42 J. Y. Kim, J. Lim, H. M. Jin, B. H. Kim, S.-J. Jeong, D. S. Choi, D. J. Li and S. O. Kim, *Advanced Materials*, 2016, **28**, 1591–1596.
- 43 J. Y. Kim, H. Kim, B. H. Kim, T. Chang, J. Lim, H. M. Jin, J. H. Mun, Y. J. Choi, K. Chung, J. Shin, S. Fan and S. O. Kim, *Nature Communications*, 2016, **7**, 12911.
- 44 J. Bai, X. Zhong, S. Jiang, Y. Huang and X. Duan, *Nat Nano*, 2010, **5**, 190–194.
- 45 T.-H. Chang, S. Xiong, R. M. Jacobberger, S. Mikael, H. S. Suh, C.-C. Liu, D. Geng, X. Wang, M. S. Arnold, Z. Ma and P. F. Nealey, *Scientific Reports*, 2016, **6**, 31407.
- 46 H. M. Jin, S. H. Lee, J. Y. Kim, S.-W. Son, B. H. Kim, H. K. Lee, J. H. Mun, S. K. Cha, J. S. Kim, P. F. Nealey, K. J. Lee and S. O. Kim, *ACS Nano*, 2016, **10**, 3435–3442.
- 47 B. H. Kim, J. Y. Kim, S.-J. Jeong, J. O. Hwang, D. H. Lee, D. O. Shin, S.-Y. Choi and S. O. Kim, *ACS Nano*, 2010, **4**, 5464–5470.
- 48 H. Zhao, W. Gu, E. Sterner, T. P. Russell, E. B. Coughlin and P. Theato, *Macromolecules*, 2011, **44**, 6433–6440.
- 49 J. Bang, S. H. Kim, E. Drockenmuller, M. J. Misner, T. P. Russell and C. J. Hawker, *J. Am. Chem. Soc.*, 2006, **128**, 7622–7629.
- 50 H. Tran, K. L. Killops and L. M. Campos, *Soft Matter*, 2013, **9**, 6578–6586.
- 51 K. L. Killops, N. Gupta, M. D. Dimitriou, N. A. Lynd, H. Jung, H. Tran, J. Bang and L. M. Campos, *ACS Macro Lett.*, 2012, **1**, 758–763.
- 52 J.-H. Ahn, H.-S. Kim, K. J. Lee, S. Jeon, S. J. Kang, Y. Sun, R. G. Nuzzo and J. A. Rogers, *Science*, 2006, **314**, 1754–1757.
- 53 M. Santhiago, J. Bettini, S. R. Araújo and C. C. B. Bufon, *ACS Appl Mater Interfaces*, 2016, **8**, 10661–10664.
- 54 M. Hamedi, R. Forchheimer and O. Inganäs, *Nat Mater*, 2007, **6**, 357–362.